

Eclipse Measurements of Io's Sodium Atmosphere

NICHOLAS M. SCHNEIDER, DONALD M. HUNTEN, WILLIAM K. WELLS,
LAURENCE M. TRAFTON

The satellites of Jupiter eclipsed each other in 1985, and these events allowed an unusual measurement of the sodium in Io's extended atmosphere. Europa was used as a mirror to look back through the Io atmosphere at the sun. The measured column abundances suggest that the atmosphere is collisionally thin above 700 kilometers and may be collisionally thin to the surface. The sodium radial profile above 700 kilometers resembles a 1500 kelvin exosphere with a surface density near 2×10^4 sodium atoms per cubic centimeter, but a complete explanation of the dynamics requires a more complex nonthermal model: the calculated loss rates suggest that the atmosphere is being replaced on a time scale of hours.

THE ATMOSPHERE OF IO IS A RESERVOIR of atoms and molecules that is continually consumed by Jupiter's plasma torus and replenished from the fresh volcanic surface (1). The satellite's atmosphere responds not only to the forces of gravity and pressure but also to a host of other processes more important at Io than at other planets: atmospheric and surface sputtering (2), atomic and ionic collisions, ionization, volcanic eruptions, atmospheric evaporation, and possibly rapid hydrodynamic escape. Each of these depends strongly on the distribution of atoms with height, but each can also drastically affect that distribution. The radial profile is an important link in our understanding of the reactions and interactions that simultaneously create and destroy the Io atmosphere. Unfortunately, the primary components, SO_2 , S, O_2 , and O, are almost undetectable from Earth.

Sodium is only a trace constituent of Io's atmosphere, but it is a strong resonant scatterer of sunlight. This effect outweighs its scarcity and makes it the most easily observed tracer of Io's extended atmosphere. The large banana-shaped sodium cloud extends many tens of Io radii ($r_{\text{Io}} = 1815$ km) and has been observed extensively since its discovery in 1973 (3). Although high-resolution spectroscopy and narrow-band imaging of sodium D-line emission (5890 Å and 5896 Å) have proven to be powerful tools for studying this phenomenon, these studies in general apply only to the outer regions of the cloud (4). Light from the region near Io includes both resonantly scattered photons

from the atmosphere and photons scattered from the bright surface. Trying to distinguish one from the other is analogous to attempting to see clouds against a snow-covered planet: there is no contrast. As a result, no reliable results can be obtained with the use of standard emission measurements near Io (5). During several eclipse events in 1985 involving Jupiter's satellites, Io's resonantly scattering sodium atmosphere cast its shadow on Europa. At these times, we were able to study Io's sodium by the absorption in Europa's spectrum instead of the emission in Io's spectrum.

A series of high-resolution spectra of Europa was taken as it swept through Io's shadow (Fig. 1), effectively scanning through Io's atmosphere at a variety of impact parameters (6, 7). Information about the two eclipses discussed here is contained in Table 1. Each spectrum contains averaged information about Io's atmosphere integrated along the solar light path. The spatial resolution is determined by the size of Euro-

pa's illuminated disk, its motion during an exposure, and the penumbral broadening of Io's shadow. The width of the resultant spatial resolution element varied from $\sim 2 r_{\text{Io}}$, far from eclipse, to $\sim 0.5 r_{\text{Io}}$ when Europa was partly in shadow.

The observations required high spectral resolving power ($\lambda/\delta\lambda \sim 5 \times 10^4$, where λ is wavelength) and telescopes large enough to obtain several good spectra during Europa's quick traverse through Io's shadow. Our best data came from the Catalina Observatory 1.5-m telescope where we used the Lunar and Planetary Laboratory Cassegrain echelle spectrograph. Additional data came from the 2.7-m McDonald Observatory telescope used at the coudé focus with an echelle spectrograph. Figure 2 shows sample spectra of Europa during and after the 14 September eclipse. The absorption features indicated by the arrows are caused by sodium along the sun-Europa line, which grazes Io. In the eight-exposure sequence, the absorption feature systematically increased as Europa neared Io's shadow, then symmetrically decreased as it receded from the other side. Each spectrum was reduced (8, 9) to a set equivalent widths (10) for the D_1 and D_2 absorption lines. Since the D_2 line is twice as optically thick as the D_1 line, both the sodium column abundance and temperature can be determined.

The data from both eclipses are plotted with theoretical curves in Fig. 3. Because the exact velocity distribution is unknown, to obtain the theoretical curves we assumed a Gaussian profile parameterized by a temperature. This assumption is supported by the good agreement between the observed line profiles and theoretical line shapes broadened by the instrumental profile. The term "temperature" is an oversimplification, since the profile includes thermal motions, bulk flow speeds, and velocities caused by collisions with the plasma. The location of

Table 1. Brief description of the eclipse parameters and the instrumentation used for two of the observed eclipses.

Parameter	Eclipse 1	Eclipse 2
Date	27 August 85	14 September 1985
Midpoint time (UT)	0602	0322
Depth of eclipse	4%	73%
Closest approach*	1.9	1.3
Time inside $10 r_{\text{Io}}$ (minutes)	310	68
Io orbital phase	47°	86°
Io magnetic longitude	1°	56°
Primary telescope	McDonald 2.7-m†	Catalina 1.5-m
Spectrograph	Coudé echelle	Cassegrain echelle
Detector	Digicon	CCD
Resolution (mÅ)	115	70
Typical integration time (minutes)	12	4.5
Typical signal-to-noise ratio	50	130

*In units of Io radius r_{Io} . Distance of closest approach refers to Europa's center of light, not its body center. †The McDonald 2.7-m telescope obtained better data this night because weather conditions at the Catalina Observatory site were marginal. The Catalina data were used as a check.

N. M. Schneider, D. M. Hunten, W. K. Wells, Lunar and Planetary Laboratory, University of Arizona, Tucson, AZ 85721.
L. M. Trafton, Astronomy Department, University of Texas, Austin, TX 78712.

each point determines the average column abundance and temperature of the spectrum. The points at the largest column abundances give the best line width information, and they indicate most probable velocities in the neighborhood of 1.2 km sec⁻¹. The velocities derived from the more distant spectra tend to be larger. Although this might be expected of distant atoms that have been subjected to more ion-atom collisions, the error bars are consistent with no change in velocity dispersion.

The two spectra from deepest eclipse rule out large isotropic expansion velocities inside about 1.5 r_{Io}. Only a small fraction of the observed sodium in this region can be traveling at velocities of more than 2 to 3 km sec⁻¹ along the line of sight. It is possible that the atmosphere is flowing primarily perpendicular to the line of sight. For the geometry of this eclipse, this is in fact the preferred direction of momentum exchange in collisions with the corotating ions (11).

In the preceding discussion we have assumed that the sodium can be described by a single velocity distribution. But Io's near-surface atmosphere is probably colder, that is, closer to the surface temperatures of 100 to 200 K. Thus our innermost spectra may include both hot and cold sodium atoms. Since the absorption lines are already broad and deep from the hot component, it is possible to add a significant amount of cold sodium without appreciably increasing the total equivalent width. We have computed spectra of 100 K sodium (characteristic velocity of 0.27 km sec⁻¹) mixed with a hot component (2.7 km sec⁻¹) and have determined that up to a factor of 10 more cold sodium can be masked by the hot component inside 1.3 r_{Io}. Outside that distance the absorption features are not as saturated and the cold component is not effectively hidden. Furthermore, our observations are not sensitive to any dense but sufficiently small (~0.1 r_{Io}) atmosphere of any temperature at the surface. In the following discussion therefore, we consider only the measurable sodium, but our conclusions will be limited by the undetectable components inside about 1.4 r_{Io}.

The atmospheric profile was constructed with the column abundances derived above and the predicted average impact parameter during an exposure (12). Figure 4 shows data from both eclipses plotted against distance from Io's center. The remarkable overlap of the data indicates that Io's atmosphere is symmetric (within a factor of 2) over two orders of magnitude in column abundance and one order of magnitude in distance. One set of points was obtained over 2 weeks before the others, most probably indicating stability over this time scale. The difference

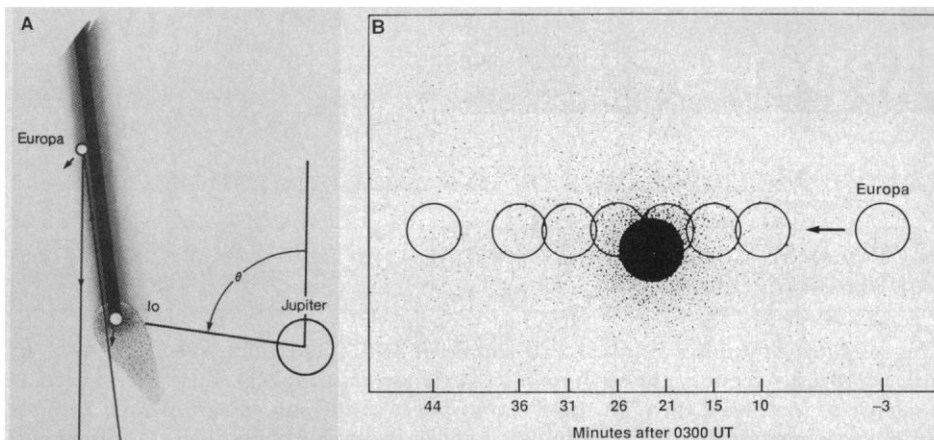


Fig. 1. Observational geometry for the eclipse of 14 September 1985. (A) Io and Europa are shown in their positions at the end of eclipse. The dark strip behind Io represents the solid body shadow of Io, and the gray shaded region schematically shows the "shadow" cast by Io's extended sodium atmosphere at the wavelength of resonant scattering. Europa, Io, and the sodium cloud are enlarged for clarity, and the penumbra is not shown.

Arrows indicate the direction and magnitude of the satellite orbital motions, and θ is Io's geocentric orbital phase angle. Although Io and Europa obviously overlap when seen from Earth owing to the 8° sun-Jupiter-Earth angle, they are separated by about 40 r_{Io} when seen from Earth owing to the 8° sun-Jupiter-Earth angle. (B) Europa's track with respect to Io's shadow on this date, as viewed from the sun. The dots represent the atmosphere, with the dot density approximately proportional to the column abundances derived from our measurements. The penumbra again is not shown: in reality both the shadow and atmosphere are blurred by about 0.5 r_{Io}. The circles indicate Europa's position at the midpoint of each observation, with the times shown below. The six innermost observations were 4.5 minutes in duration, and the other two were 10.0 minutes. Sodium absorption was detected in all eight exposures.

in magnetic longitude between the two eclipses is too small to determine any dependence on this parameter.

A least-squares power law fit to the data is plotted in Fig. 4 (line A). The estimated sodium column abundance N (in atoms per square centimeter) at any impact parameter b is $N(b) = (2.0 \pm 0.7) \times 10^{12} \times b^{-(2.1 \pm 0.6)}$. This is the integral through an atmosphere whose local sodium density n (in atoms per cubic centimeter) at radius r is $n(r) = (6000 \pm 2000) \times r^{-(3.1 \pm 0.6)}$, where b and r are in units of Io radii. As discussed above, these equations are probably not applicable below 1.3 r_{Io}.

The data show Io's atmosphere to be surprisingly "well behaved," falling off according to a power law out to ten planetary radii. But over much of this range it can scarcely be called Io's atmosphere. Jupiter's gravity dominates outside 5.6 r_{Io}, and the sodium atoms are far more likely to collide with a torus ion or electron than with another atom or the surface. Standard atmospheric models do not apply here, but for the sake of comparison we discuss here two simplistic cases.

Each model is described by a spherically symmetric density function, which is integrated along lines of sight to derive column abundances. Line B in Fig. 4 shows a power law column abundance distribution with exponent -1 (local density $\propto 1/r^2$). This is the dependence observed by Trafton and

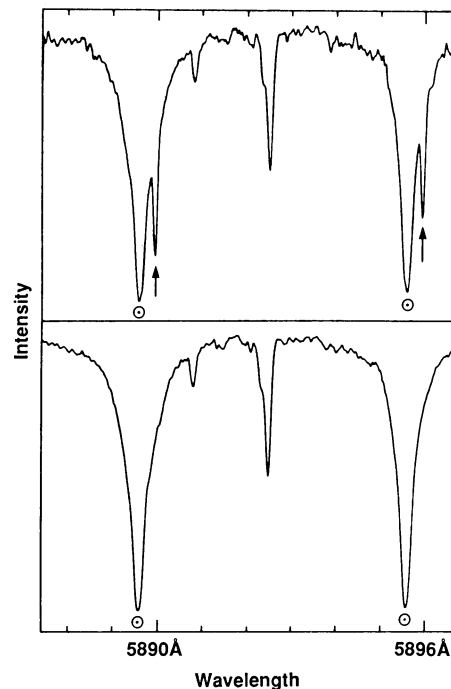
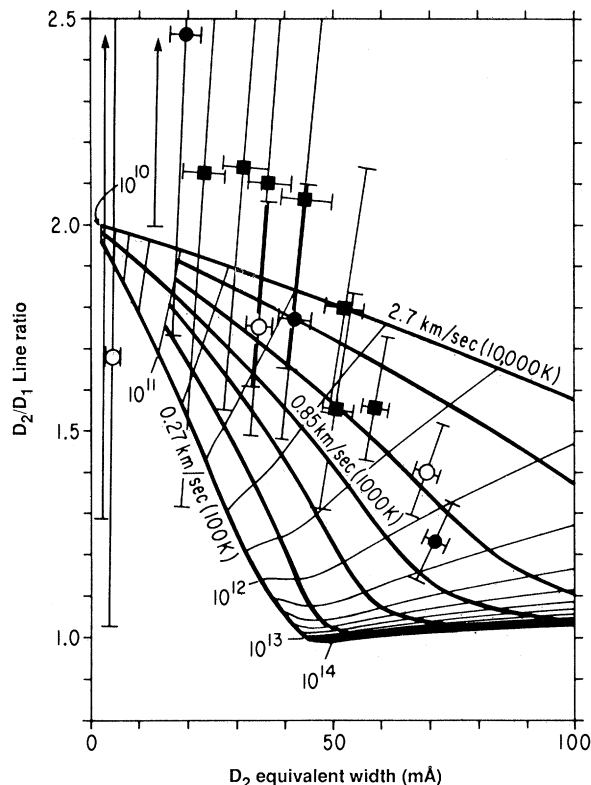


Fig. 2. Processed spectra of Europa on 14 September 1985. (Top) Near eclipse minimum, 0326 UT; and (bottom) after the eclipse, 0407 UT. The broad absorption features marked \odot are caused by sodium in the sun's atmosphere. The arrows indicate absorption features that have appeared on the red side of the solar absorption, with the Doppler shift indicating that the sodium is moving toward the sun with Io's velocity. Note that the D₂ absorption (left absorption line) is slightly stronger than the D₁ feature. The top spectrum is noisier because the exposure was shorter and Europa was about half eclipsed.

Fig. 3. Combined equivalent-width calculations for the D_1 and D_2 lines. The bold lines show the dependence of equivalent width and line ratio for temperatures of 100, 200, 500, 1,000, 2,000, 5,000, and 10,000 K. The most probable velocities for several of these temperatures are given. The lighter lines represent column abundance contours in units of sodium atoms per square centimeter. Each data set sampled the atmosphere above a different region of Io: (●) above the Jupiter-facing hemisphere (central Io longitude 0°); (○) above the anti-Jupiter hemisphere (180°); and (■) above the hemisphere 45° outside the leading hemisphere (135°). The error bars show the primary axes of the 90% confidence error ellipse constructed from the measurement errors.



Macy (13) in the range of 20 to 200 r_{10} , which was interpreted as evidence for a radially streaming atmosphere that flows without losses and without slowing. The new data do not follow a simple streaming model over the range 1 to 10 r_{10} ; the addition of ionization losses to the model and choice of a suitable flow velocity would yield a better match to the data.

Atoms in the upper part of an atmosphere (the exosphere) experience few collisions with other atoms, whereas atoms are assumed to be in thermal equilibrium at the bottom boundary (the exobase). Above the exobase, the atoms travel on ballistic trajectories without collisions. Curve C in Fig. 4 represents a 1500 K exosphere with a sodium density at the surface of 2×10^4 atoms per cubic centimeter. This curve closely resembles two recent models by Summers *et al.* and McGrath and Johnson (14), assuming a 1% sodium mixing ratio and an exobase at or near the surface. The curve matches the data acceptably over the entire range, but the model does not include important effects such as Jupiter's gravity and all the interactions with the corotating plasma. A more realistic case would include ionization losses and bulk outflow velocities. More complex models are required, but these examples might serve as useful starting points.

One of the important unresolved issues of the Io atmosphere is the location of the exobase. If it is coincident with the surface, magnetospheric ions may be able to directly

bombard the surface, and the ejected atoms can escape directly to space. If, on the other hand, the exobase lies $\sim 1r_{10}$ above the surface, then the atmosphere presents a target for bombardment that is four times the area of Io alone, and the surface and lower atmosphere are protected. The exobase location will be determined by the dominant constituents, however, not sodium. The integrated density of oxygen, sulfur, and SO_2 above the exobase must be $\sim 3 \times 10^{14}$ atoms per square centimeter (15). If we assume that sodium makes up 1% of the atmosphere (16), the total integrated density above the surface implied by the data is only 6×10^{13} atoms per square centimeter. Even if we allow the maximum amount permitted by the error bars of the coldest imaginable sodium (100 K), the integrated density falls below the critical value near $1.4 r_{10}$. This forces one of two results: either the fraction of atomic sodium is much less than 1%, or the exobase is below $1.4 r_{10}$. Given the assumptions made, we suspect the exobase is even lower. Nothing in our data precludes the possibility that the exobase is coincident with the surface.

Sodium in the observed range is depleted by three major processes: electron impact ionization, transport out of the region, and charge exchange (17), and using the best-fit model, we can calculate approximate rates for each. The power law fit gives a total of about 10^{30} sodium atoms between 1 and 10 r_{10} , excluding the region shadowed by Io's

disk. The ionization lifetime near Io is typically ~ 2 hours (1), giving a loss rate of $\sim 10^{26}$ atoms per second. This rate would increase substantially if a thick undetectable component exists near the surface. It would decrease if the atmosphere is protected by intrinsic magnetic fields, diversion of plasma flow, or cooling of the ionizing electrons.

A calculation of the sodium transport rate requires knowledge of the velocities in the outer part of the observed region (5 to 10 r_{10}). This region must be replenished on the time scale of an ionization lifetime, so velocities of at least 2 km sec^{-1} are required there. If this is used as an expansion velocity, the rate of transport of neutral sodium across the 10 r_{10} boundary is $\approx 5 \times 10^{25}$ atoms per second, giving an atmospheric lifetime of at most ~ 6 hours. It is difficult to compare these calculations with previous ones (1, 2) that combine ionization and transport rates, but to first order they are consistent.

Finally, we calculate the rate for charge exchange, the process responsible for creating the high-speed jets observed from Earth (17). From the atmospheric inventory derived above, the supply rate to these jets is $\sim 10^{24}$ atoms per second, for a 1% sodium-ion mixing ratio. Analysis of the jet observations may prove to be quite powerful: charge exchange is the only directly measurable loss process and may indicate either the presence of a near-surface component or the existence of a shielding mechanism.

One of the remarkable traits of the well-studied sodium cloud outside 10 r_{10} is its stability over time scales of hours to years,

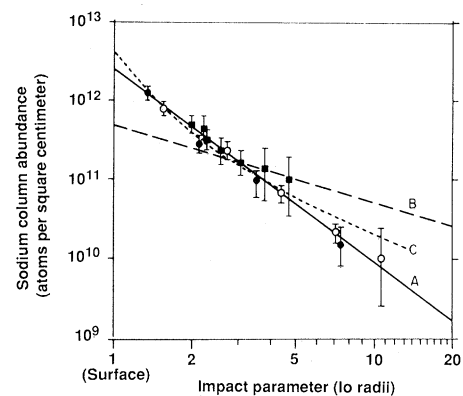


Fig. 4. The determined column abundances are plotted versus average impact parameter from Io's center. The vertical error bars show the propagated errors from the observed quantities but do not include the possible existence of a cold component. Each measurement was made over a range of impact parameters, because of Europa's size and motion. The spatial resolution element was typically $1.2 r_{10}$ across but varied with the phase of eclipse and integration time. The error in the centroid is $\sim 0.05 r_{10}$ and is not shown. The column abundances beyond $\sim 8 r_{10}$ were confirmed by means of simultaneously obtained standard emission spectra.

even though Io's plasma environment shows large variations. This suggests the existence of some protected reservoir. The calculations above show that the lifetime of the inventory in the range $\sim 1 \tau_{10}$ to $10 \tau_{10}$ is too short to perform that function. The surface itself or a dense atmosphere inside $1.4 \tau_{10}$ may be acting as a buffer.

REFERENCES AND NOTES

1. A review of our current understanding of Io and the major unresolved questions appears in several chapters of *Satellites*, J. A. Burns and M. S. Matthews, Eds. (Univ. of Arizona Press, Tucson, 1986).
2. The sputtering process involves the impact of high-energy ions on a surface or thick atmosphere, and the subsequent release and ejection of high-speed atoms and molecules over a range of velocities. See the review by A. F. Cheng, P. K. Haff, R. E. Johnson, and L. J. Lanzerotti in (1), p. 403. This chapter also includes estimates of the supply rates to the torus and neutral clouds.
3. The emission was discovered by R. A. Brown [in *Exploration of the Planetary System*, A. Woszczyk and C. Iwaniszewska, Eds. (Reidel, Dordrecht, 1974), p. 527]. L. Trafton, T. Parkinson, and W. Macy [*Astrophys. J.* **190**, L85 (1974)] determined that the emission came from an extended region around Io.
4. B. A. Goldberg *et al.*, *Science* **226**, 512 (1984).
5. R. A. Brown, R. M. Goody, F. J. Murcray, *Astrophys. J.* **200**, L49 (1975).
6. Five eclipses were successfully observed, but we discuss only two. Eclipse 1 was only grazing: Europa slowly approached Io's shadow from the east, barely touched it, and then receded again to the east. Eclipse 2 was deep but fast: Europa passed rapidly through the shadow from west to east. Favorable eclipses were also observed on 15, 21, and 23 September 1985 (see N. M. Schneider, thesis, University of Arizona, in preparation). The eclipse series occur every 6 years [K. Aksnes and F. Franklin, *Icarus* **60**, 180 (1984); and J. E. Arlot, *Astron. Astrophys.* **138**, 113 (1984)].
7. The term impact parameter is defined as the perpendicular distance between the incident solar beam of light and Io's center.
8. The Catalina Observatory data are spatially resolved CCD (charge-coupled device) spectra with Io and Europa simultaneously recorded. The rows spanning Europa's spectrum were weighted according to noise and summed for collapse to one dimension. Terrestrial water lines were removed by means of the spectrum of a rapidly rotating B-star, and the solar lines were eliminated by dividing by a similarly corrected spectrum of Europa far from eclipse. Equivalent widths were measured digitally by summing over the absorption feature. The primary error stems from the subjective placement of the continuum. Error bars are estimated 90% confidence intervals.
9. The McDonald Observatory data are one-dimensional spectra of Europa. The solar and telluric lines were removed with a combination of lunar and Ganymede spectra. Equivalent widths were determined by approximating the absorption feature by a triangle and measuring the area relative to the continuum. A subset of the simultaneous Catalina Observatory data was reduced, and the results were used in the final determination of the error bars.
10. The equivalent width W is defined as the integral over the normalized spectrum of the difference between the continuum and the absorption feature. The result is in units of wavelength, in this case milliangstroms (mÅ). It is the width of a completely saturated absorption feature whose W matches the observed line.
11. E. M. Sievcka and R. E. Johnson, *Astrophys. J.* **287**, 418 (1984).
12. J. H. Lieske of the Jet Propulsion Laboratory provided the ephemeris listing of satellite positions corrected for light-time. These positions were input to an eclipse-simulating program that calculated the apparent center of light of Europa during eclipse.

13. L. Trafton and W. Macy, *Icarus* **33**, 322 (1978).
14. Summers *et al.* constructed a Chamberlain-type exosphere similar to the one used here (M. E. Summers, D. F. Strobel, Y. L. Yung, J. T. Trauger, F. Mills, in preparation). M. A. McGrath and R. E. Johnson [*Icarus* **69**, 519 (1987)] generated a corona around Io by modeling the ballistic trajectories of atoms and molecules ejected by sputtering from the exobase.
15. The exobase is defined as the location from which a high-speed atom has a 1/e chance of escaping without colliding with another atom. Using a typical collision cross section $\sigma = 30 \text{ \AA}^2$, we calculate the appropriate integrated density $1/\sigma = 3 \times 10^{14} \text{ cm}^{-2}$.
16. Only two measurements of the sodium mixing ratio near Io have been made, both involving Voyager ion experiments. The upper limit of sodium in the cold torus plasma is estimated at $\leq 5\%$ [F. Bagenal and J. D. Sullivan, *J. Geophys. Res.* **86**, 8447 (1981)]. N. Gehrels and E. Stone [*ibid.* **88**, 5537 (1983)] measured a 3% sodium mixing ratio with the low-energy telescope experiment. One effect that can reduce neutral sodium's local mixing ratio is its short lifetime against ionization; sodium at a distance of several τ_{10} could be depleted by up to a factor of 10 compared to other constituents.
17. In a charge-exchange reaction, a high-speed ($\sim 57 \text{ km sec}^{-1}$) sodium ion accepts an electron from a sodium atom, thereby becoming a fast neutral. The cross section for this reaction is $\sim 150 \text{ \AA}^2$. Jets of these neutrals have been reported by J. T. Trauger [*Bull. Am. Astron. Soc.* **16**, 712 (1984) (abstr.)] and N. M. Schneider, D. M. Hunten, and R. A. Brown [*ibid.* (abstr.), p.663].
18. We thank U. Fink, A. B. Schultz, and M. A. DiSanti for providing and operating the CCD camera for the Lunar and Planetary Laboratory echelle spectrograph; J. H. Lieske, F. A. Franklin, and K. Aksnes for ephemeris calculations; R. A. Tucker for observing assistance; and R. L. Marcialis, J. R. Spencer, and E. Karkoshka for photometric support. R. V. Yelle provided the exospheric calculations. N.M.S., D.M.H., and W.K.W. acknowledge the support of NASA grant NAGW-596 and L.M.T. acknowledges NASA grant NGR44-012-152. The CCD is operated under NASA grant NSG 7070. We thank R. A. Brown, W. H. Smyth, and M. E. Summers for drawing our attention to the eclipses in the first place.

27 February 1987; accepted 7 July 1987

Electromagnetic Stabilization of Weakly Conducting Fluids

CORNELIUS F. IVORY,*† WILLIAM A. GOBIE, JAMES B. BECKWITH, ROBERT HERGENROTHER, MICHAEL MALEC

Classical hydromagnetic theory predicts that the flow of dilute aqueous electrolyte in a slit can be stabilized by application of a strong, transverse magnetic field. However, recent experiments indicate that stabilization can be achieved with the use of a much weaker field in the presence of a small lateral current. A revised theory describes how the magnetic and electric fields interact to eliminate natural convection.

WHEN A HORIZONTAL LIQUID film is heated uniformly from below, a patterned flow consisting of spatially periodic rolls or cells (Fig. 1) may develop if the temperature gradient, ∇T , causes the Rayleigh number

$$Ra \equiv \frac{\rho g \beta |\nabla T| h^4}{\eta \kappa} \quad (1)$$

to exceed its critical value. In this expression $\rho(T)$ is the density, g is the gravitational acceleration, β is a thermal expansion coefficient, h is the thickness of the film, η is the viscosity, and κ is the thermal diffusivity of the fluid. For a horizontal slit bounded by perfectly conducting walls this critical value is $Ra_c \approx 1708$ (1).

A related instability occurs if the slit is oriented vertically while maintaining the temperature gradient parallel to gravity. For example, consider a chamber (Fig. 2) in which a thin film of electrolyte is heated by

an electric current. In this case experiments conducted at Ra slightly higher than the

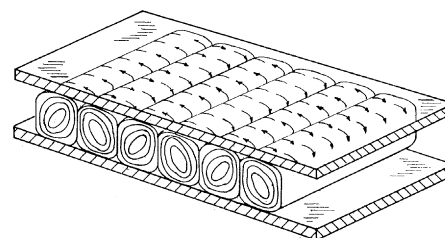
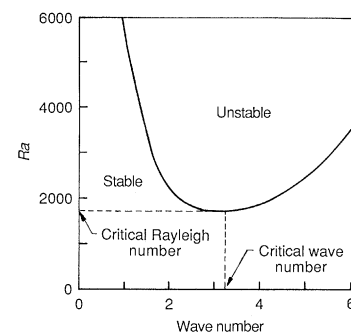


Fig. 1. Natural convection in a horizontal film heated from below is sometimes evident as spatially periodic rolls or cells. Convection may occur when the Rayleigh number exceeds its critical value, in this case $Ra_c \approx 1708$.

Department of Chemical Engineering, University of Notre Dame, Notre Dame, IN 46556.

*To whom correspondence should be addressed.
†Present address: Department of Chemical Engineering, Washington State University, Pullman, WA 99164.